Linear analysis of generalized turbulent hyperbolic flow in a rotating frame

C. A. Langer, E. Akylas,[a] and S. C. Kassinos[b]
Department of Mechanical and Manufacturing Engineering, University of Cyprus, Nicosia 1678, Cyprus

(Received 6 September 2007; accepted 30 October 2007; published online 26 December 2007)

We apply inviscid rapid distortion theory to the generalized case of turbulent hyperbolic flow in a rotating frame and investigate the dependence of the evolution of the turbulent kinetic energy on the frame rotation rate. We derive an analytical two-dimensional solution which allows for an accurate approximation of the three-dimensional initially isotropic problem. From the analytical solutions we determine a new generalized stability criterion for the evolution of the turbulent kinetic energy in this class of flows. © *2007 American Institute of Physics*. [DOI: 10.1063/1.2821911]

In this study we follow the methodology presented in Ref. 1 and we generalize the respective solution for any hyperbolic flow. We show that the turbulence in the hyperbolic cases tends to align at least with one well-specified axis (defining the eddy-axis system), which means that the turbulence becomes independent of the corresponding direction. We derive analytical spectral solutions, at this particular two-dimensional (2D) limit, for the fluctuating velocity components. The subsequent analysis of the stresses yields the correct stability criterion for the evolution of the turbulent kinetic energy (TKE). The solutions are validated by comparison with the three-dimensional (3D) numerical results, calculated using the particle representation model (PRM).[2–4] In the case of a generalized hyperbolic flow with frame rotation, the mean strain rate, mean rotation rate, and frame rotation rate tensors in the laboratory $\tilde{x}_i$ reference frame are

$$\tilde{S}_{ij} = \Gamma(\delta_{i1}\delta_{j2} + \delta_{i2}\delta_{j1}), \quad \Omega_{ij} = \varepsilon_{ij3}\Omega, \quad \Omega^f_{ij} = \varepsilon_{ij3}\Omega^f, \quad (1)$$

with $|\Gamma| \geqslant |\Omega|$. The value $\Omega=0$ corresponds to the lower limiting case of the plane strain flow, while $\Omega=\Gamma$ determines the upper limiting pure shear flow case. The linear rapid distortion theory (RDT) equations for the evolution of the fluctuating velocity components $\tilde{u}_i(\tilde{x}_1,\tilde{x}_2,\tilde{x}_3)$ in this reference frame are

$$\frac{\partial \tilde{u}_i}{\partial t} = -(\Gamma+\Omega)\left(\tilde{x}_2\frac{\partial \tilde{u}_i}{\partial \tilde{x}_1} + \delta_{i1}\tilde{u}_2\right) - (\Gamma-\Omega)\left(\tilde{x}_1\frac{\partial \tilde{u}_i}{\partial \tilde{x}_2} + \delta_{i2}\tilde{u}_1\right) - \frac{1}{\rho}\frac{\partial p}{\partial \tilde{x}_i} + 2\varepsilon_{ij3}\Omega^f\tilde{u}_j. \quad (2)$$

As will be shown, in hyperbolic flows the evolution of the turbulence under RDT is such that it approaches a two-dimensional state. More specifically, turbulent eddies align with a specific direction and the fluctuating velocities become independent of this particular direction. For the subsequent analysis we choose a coordinate system aligned with this direction of independence, the eddy-axis system. This allows for a simplified 2D analysis, following the methodology presented in Ref. 1 for plane strain flow. We determine the eddy-axis system by looking at the final orientation of evolving material lines.[5] Taking the evolution of a material line ℓ_i (Refs. 5–7), we find the evolution equation of the eddy-axis vector $a_i=\ell_i/\ell$

$$\mathrm{d}a_i/\mathrm{d}t = \mathrm{d}(\ell_i/\ell)/\mathrm{d}t = G_{ik}a_k - ba_i, \quad (3)$$

where ℓ is the magnitude. Setting $da_i/dt=0$ in Eq. (3), we derive the fixed orientation of the material line, determining the axis of independence, as

$$b^2 = \Gamma^2 - \Omega^2, \quad a_1 = \sqrt{\frac{\Gamma+\Omega}{2\Gamma}}, \quad a_2 = \sqrt{\frac{\Gamma-\Omega}{2\Gamma}}. \quad (4)$$

We transform now Eqs. (1) and (2) from the laboratory reference frame $(\tilde{x}_1,\tilde{x}_2,\tilde{x}_3)$, into the new eddy-axes coordinates. Noting that a_1 and a_2 are direction cosines, the coordinate transformation follows

$$\begin{aligned} x_1 &= a_1\tilde{x}_1 + a_2\tilde{x}_2, \quad x_2 = -a_2\tilde{x}_1 + a_1\tilde{x}_2, \quad x_3 = \tilde{x}_3, \\ u_1 &= a_1\tilde{u}_1 + a_2\tilde{u}_2, \quad u_2 = -a_2\tilde{u}_1 + a_1\tilde{u}_2, \quad u_3 = \tilde{u}_3, \end{aligned} \quad (5)$$

and the mean gradients transform to (note that the transformation does not modify the rotation tensors, since the rotation is around the x_3 axis)

$$S_{ij} = \Omega(\delta_{i1}\delta_{j2} + \delta_{i2}\delta_{j1}) + \sqrt{\Gamma^2-\Omega^2}(\delta_{i1}\delta_{j1} - \delta_{i2}\delta_{j2}). \quad (6)$$

In the eddy-axes coordinates, S_{ij} is diagonal. From Eq. (6) it follows that for the limiting pure shear case $(\Gamma=\Omega)$ the transformed coordinates coincide with the initial reference frame, while for the limiting plane strain case $(\Omega=0)$ the transformed coordinates are turned by $\pi/4$. In the new coordinate system, the three-dimensional and three-component (3D-3C) linear equations for the fluctuating momentum are

$$\frac{\partial u_i}{\partial t} = -2\Omega\left(\delta i_1 u_2 + x_2\frac{\partial u_i}{\partial x_1}\right) - \sqrt{\Gamma^2-\Omega^2}\left(\delta_{i1}u_1 - \delta_{i2}u_2 + x_1\frac{\partial u_i}{\partial x_1} - x_2\frac{\partial u_i}{\partial x_2}\right) - \frac{1}{\rho}\frac{\partial p}{\partial x_i} + 2\varepsilon_{ij3}\Omega^f u_j. \quad (7)$$

For $\Gamma=\Omega$, Eq. (7) corresponds to the pure shear case,[8] with $S=2\Gamma=2\Omega$, while for $\Omega=0$, Eq. (7) reduces to Eq. (2.5) in

[a]Also with the Institute of Environmental Research, National Observatory of Athens, Greece.
[b]Also with the Center for Turbulence Research, Stanford University/NASA-Ames. Author to whom correspondence should be addressed. Electronic mail: kassinos@ucy.ac.cy.

Ref. 1 for plane strain turbulent flow. Using the Rogallo[9–11] transformation, we set

$$\xi_i = \delta_{i1}\left(x_1 e^{-\Gamma^* t} - x_2 \frac{2\gamma}{\sqrt{1-\gamma^2}}\sinh(\Gamma^* t)\right) + \delta_{i2} x_2 e^{\Gamma^* t} + \delta_{i3} x_3, \tag{8}$$

where $\gamma = \Omega/\Gamma \leqslant 1$ and $\Gamma^* = \Gamma\sqrt{1-\gamma^2}$, and Eq. (7) transforms to

$$\begin{aligned}\frac{\partial u_i}{\partial t} &= \Gamma^* \delta_{i2} u_2 - \delta_{i1}(2\Omega u_2 + \Gamma^* u_1) + 2\varepsilon_{ij3}\Omega^f u_i \\ &\quad - \frac{1}{\rho}\left[\frac{\partial p}{\partial \xi_i}(\delta_{i1} e^{-\Gamma^* t} + \delta_{i2} e^{\Gamma^* t} + \delta_{i3})\right. \\ &\quad \left. - \delta_{i2}\frac{\partial p}{\partial \xi_1}\frac{2\gamma \sinh(\Gamma^* t)}{\sqrt{1-\gamma^2}}\right],\end{aligned} \tag{9}$$

Applying the Fourier transformation to Eq. (9), the Fourier coefficients (denoted with ˆ) for the fluctuating velocity components in spectral space evolve as

$$\frac{\partial \hat{u}_i}{\partial t} = i\frac{\hat{p}}{\rho}k_i - 2\Omega\delta_{i1}\hat{u}_2 - \Gamma^*(\delta_{i1}\hat{u}_1 - \delta_{i2}\hat{u}_2) + 2\varepsilon_{ij3}\Omega^f \hat{u}_j, \tag{10}$$

where due to the deformation applied, the wave numbers evolve as

$$k_i = \delta_{i1} k_1^0 e^{-\Gamma^* t} + \delta_{i2}\left(k_2^0 e^{\Gamma^* t} - k_1^0 \frac{2\gamma}{\sqrt{1-\gamma^2}}\sinh(\Gamma^* t)\right) + \delta_{i3} k_3^0, \tag{11}$$

where the superscript "0" denotes initial values. From Eq. (11) it is clear that in the generalized hyperbolic case the wave number component $k_1^0 e^{-\Gamma^* t}$ vanishes with time (Fig. 3) and thus, the turbulence approaches a state which is independent of the x_1 axis in the eddy-axis frame. Introducing the 2D Fourier mode with $k(k_1=0, k_2, k_3)$, similar to Ref. 1, the system (10) simplifies

$$\begin{aligned}&\partial\hat{u}_1/\partial t = -2\Omega\hat{u}_2 - \Gamma^*\hat{u}_1 + 2\Omega^f\hat{u}_2, \\ &\partial\hat{u}_2/\partial t = \Gamma^*\hat{u}_2 + i\hat{p}k_2 e^{\Gamma^* t}/\rho - 2\Omega^f\hat{u}_1, \quad \partial\hat{u}_3/\partial t = i\hat{p}k_3/\rho.\end{aligned} \tag{12}$$

Applying the Fourier transformed continuity equation, $k_2 e^{\Gamma^* t}\hat{u}_2 + k_3\hat{u}_3 = 0$, we can solve for the pressure, resulting in

$$\frac{\partial \hat{u}_1}{\partial \beta^*} = 2\frac{(\Omega^f - \Omega)}{\Gamma^*}\hat{u}_2 - \hat{u}_1,$$

$$\frac{\partial \hat{u}_2}{\partial \beta^*} = \frac{k_3^2\hat{u}_2 - k_2^2 e^{2\beta^*}\hat{u}_2 - \dfrac{2\Omega^f}{\Gamma^*}k_3^2\hat{u}_1}{k_2^2 e^{2\beta^*} + k_3^2}, \tag{13}$$

$$\frac{\partial \hat{u}_3}{\partial \beta^*} = k_2 k_3 \frac{\dfrac{2\Omega^f}{\Gamma^*}e^{\beta^*}\hat{u}_1 - 2e^{\beta^*}\hat{u}_2}{k_2^2 e^{2\beta^*} + k_3^2},$$

where $\beta^* = \Gamma^* t$. Furthermore, we set $\theta^2 = k_2^2/k_3^2$ and $\eta_*^2 = 4\Omega^f(\Omega^f - \Omega)/\Gamma_*^2$, and after some algebra, the system of equations (13) yields the uncoupled forms

$$(1+\theta^2 e^{2\beta^*})\frac{\partial^2\hat{u}_1}{\partial\beta^{*2}} + 2\theta^2 e^{2\beta^*}\frac{\partial\hat{u}_1}{\partial\beta_*} + (\eta^{*2} - 1 + \theta^2 e^{2\beta^*})\hat{u}_1 = 0,$$

$$\hat{u}_3 = -\theta e^{\beta^*}\hat{u}_2, \tag{14}$$

$$(1+\theta^2 e^{2\beta^*})\frac{\partial^2\hat{u}_2}{\partial\beta^{*2}} + 4\theta^2 e^{2\beta^*}\frac{\partial\hat{u}_2}{\partial\beta_*} + (\eta^{*2} - 1 + 3\theta^2 e^{2\beta^*})\hat{u}_2 = 0,$$

Equations (14) are the same as the respective equations (4.3) obtained in Ref. 1 for plane strain turbulent flow in a rotating frame. Consequently the general solution of Eq. (14) is exactly the same as the general solution in Ref. 1 for the plane strain case [their Eq. (4.10)]

$$\hat{u}_1 = \frac{e^{\beta\sqrt{1-\eta^{*2}}}[(A_1^+\hat{u}_1^0 + A_2^+\hat{u}_2^0) - e^{-2\beta^*\sqrt{1-\eta^{*2}}}(A_1^-\hat{u}_1^0 + A_2^-\hat{u}_2^0)]}{A(\sin^2\varphi + e^{2\beta^*}\cos^2\varphi)^{1/2}},$$

$$\hat{u}_2 = \frac{e^{\beta^*\sqrt{1-\eta^{*2}}}[(B_1^+\hat{u}_1^0 + B_2^+\hat{u}_2^0) - e^{-2\beta^*\sqrt{1-\eta^{*2}}}(B_1^-\hat{u}_1^0 + B_2^-\hat{u}_2^0)]}{B(\sin^2\varphi + e^{2\beta^*}\cos^2\varphi)^{1/2}}, \tag{15}$$

$$\hat{u}_3 = -e^{\beta^*}\cot\varphi\hat{u}_2.$$

However, the generalized initial conditions are slightly different compared to the ones in Ref. 1,

$$\begin{aligned}\left.\frac{\partial\hat{u}_1}{\partial\beta^*}\right|_{\beta^*=0} &= \frac{(\eta - 2\gamma)}{\sqrt{1-\gamma^2}}\hat{u}_2^0 - \hat{u}_1^0, \\ \left.\frac{\partial\hat{u}_2}{\partial\beta^*}\right|_{\beta^*=0} &= \frac{(1-\theta^2)\hat{u}_2^0 - (\eta/\sqrt{1-\gamma^2})\hat{u}_1^0}{1+\theta^2},\end{aligned} \tag{16}$$

and thus, $A_2^\pm$ and $B_1^\pm$ in Eqs. (15) are slightly modified as $A_2^\pm = A_{2\mathrm{PS}}^\pm(\eta - 2\gamma)/\sqrt{1-\gamma^2}$, $B_1^\pm = B_{1\mathrm{PS}}^\pm\eta/\sqrt{1-\gamma^2}$, where the subscript "PS" refers to the solutions (4.10) in Ref. 1. The parameters $a_\pm$ in the corresponding hypergeometric functions, depending on η^{*2} as $a_\pm = (1 \pm \sqrt{1-\eta^{*2}})/2$. The limit of the solutions (15) when $\varphi = \pi/2$, is identical to the one-dimensional (1D) pressureless analysis limit,[1] where the equations result in an exponential growth of the TKE with time, for $\eta^{*2} < 1$. For values of η^{*2} larger than 1, the stresses (at this pressureless 1D limit) oscillate and the TKE stabilizes around a constant value. The same criterion for the stabilization of the TKE has been reported in Ref. 12 based on their pressureless analysis of a generalized quadratic flow. However, as shown in Ref. 1 for the plane strain case, the contribution of the whole range of φ must be taken into account. More specifically, as φ departs from $\pi/2$ towards $\varphi = 0$ or $\varphi = \pi$, the Fourier coefficients decrease symmetrically. At exactly $\varphi = 0$ or $\varphi = \pi$, the solution becomes inde-

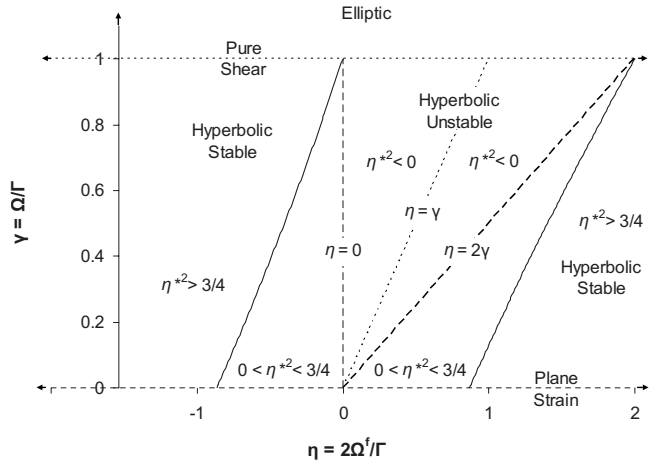

FIG. 1. The dependence of the turbulence stability on the governing parameters η and γ, for a general hyperbolic flow in a rotating frame. The solid lines ($\eta^{*2}=3/4$) bound the unstable regime and the long dashed lines ($\eta^{*2}=0$) determine the range of the negative values for η^{*2}. In the latter the energy growth peaks when $\eta=\gamma$ (short dashed line).

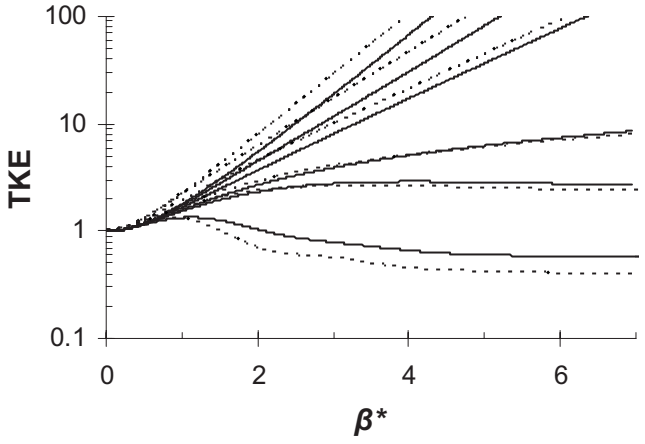

FIG. 2. Evolution of the TKE, normalized by its initial value, for the initially homogeneous 3D case calculated numerically with the PRM (solid) and the 2D analysis presented here (dashed) for $\gamma=0.5$ and $\eta^{*2}=-1/3$, 0, 0.5, 0.75, 1, and 3.35 (clockwise).

pendent of the frame rotation rate, in agreement with the principle of *material indifference*[13] for 2D turbulence independent of the axis of the frame rotation ($k_3=0$). This shows that the Fourier modes approach constant values; the fluctuations do not grow with time. As in the case of plane strain,[1] the contribution of the full φ range, i.e., $0\leqslant\varphi\leqslant\pi$, modifies markedly the TKE evolution and, as a result, also modifies the stability limits compared to the pressureless approach. Following similar arguments as presented in Ref. 1 for the plane strain case, and applying the same way the steepest descent analysis method, it becomes clear that for values of $\eta^{*2}\leqslant 1$, when the parameters $a_\pm$ are real numbers, the Reynolds stress components R_{11}, R_{22}, R_{33}, and R_{12} (and consequently the TKE) resulting from the integration of the spectral relations over all wave numbers, approach quickly the following exponential behavior: $R_{ij}\sim\exp[\beta^*(2\sqrt{1-\eta^{*2}}-1)]$. For values of $\eta^{*2}>1$, the parameters $a_\pm$ are complex numbers, resulting in the stabilization of the energy showing damped oscillations, with a period proportional to $(\eta^{*2}-1)^{-1/2}$. As a result of the 2D analysis, the stability criterion for a generalized hyperbolic flow is $\eta^{*2}\leqslant 3/4$, which, in terms of the governing parameters γ and η, shows that the unstable hyperbolic cases are located in the range (Fig. 1):

$$\gamma-\sqrt{3+\gamma^2}/2\leqslant\eta\leqslant\gamma+\sqrt{3+\gamma^2}/2. \tag{17}$$

Outside this range, the TKE stabilizes. The unstable regime shown in Fig. 1 can be divided in two well defined regions. For values of $0<\eta^{*2}<3/4$ we can connect the results directly to the solutions for plane strain for the same η^*. Using vortical and jetal initial turbulence,[1] Eqs. (15) show, respectively, that

$$R_{\alpha\beta}(\beta^*)=A_{\alpha\beta}R_{\alpha\beta,\mathrm{PS}}(\beta_{\mathrm{PS}}=\beta^*,\eta_{\mathrm{PS}}=\eta^*) \tag{18}$$

(no summation implied by repeated greek indices), where for the vortical cases $A_{11}^{\mathrm{vor}}=1-2\gamma/\eta$, $A_{22}^{\mathrm{vor}}=A_{33}^{\mathrm{vor}}=1$, and $A_{12}^{\mathrm{vor}}=\sqrt{A_{11}^{\mathrm{vor}}}$, while for the jetal cases $A_{11}^{\mathrm{jet}}=1$, $A_{22}^{\mathrm{jet}}=A_{33}^{\mathrm{jet}}=(1-2\gamma/\eta)^{-1}$, and $A_{12}^{\mathrm{jet}}=\sqrt{A_{22}^{\mathrm{jet}}}$. Note that the dimensionless time β^* in the solutions for the generalized hyperbolic flow corresponds to the dimensionless time β_{PS} in the specific solution for the plane strain case. For Eq. (18), it can be shown that the long time asymptotic states for the componentality of the turbulence, in the eddy-axes coordinates, which is described by the normalized stresses $r_{ij}=R_{ij}/R_{kk}$, are linked to the respective ones for the corresponding plane strain cases (Table I in Ref. 1) through

$$r_{\alpha\beta}=\frac{A_{\alpha\beta}^{\mathrm{vor}}r_{\alpha\beta,\mathrm{PS}}(\eta-2\gamma)/\eta}{r_{11,\mathrm{PS}}(\eta-2\gamma)/\eta+r_{22,\mathrm{PS}}+r_{33,\mathrm{PS}}}, \tag{19}$$

When $\eta^{*2}<0$, there is no such connection because there is no plane strain case corresponding to negative η^{*2}. In this range, the energy growth increases (following the increase of the parameter $2\sqrt{1-\eta^{*2}}$, in the exponents) and peaks for $\eta=\gamma$, when η^{*2} takes the largest negative values. In Fig. 2 we present a comparison between the TKE evolution calculated by the analytical expressions derived here using the initially 2D-3C case with $k_1=0$, and the numerical solution for the 3D-3C initially isotropic case calculated using the PRM,[2–4] with large enough number of particles to ensure the accuracy of the solution. The 2D results are presented for a $2/3-1/3$ weighted superposition between the vortical and the jetal initializations, respectively. This corresponds to an initial equipartition of the energy: $r_{11}=r_{22}=r_{33}=1/3$. From the comparison it turns out that the 2D solution explains accurately the type of the TKE growth, identifying the parameter $-1+2\sqrt{1-\eta^{*2}}$ as the criterion for the stability of the turbulent flow. Starting with the most unstable case (for $\eta^{*2}=-1/3$), we notice a strong exponential evolution with time, which is of the form $\sim\exp[(-1+2\sqrt{1-\eta^{*2}})\beta^*]$. As η^{*2} increases the exponential growth becomes less pronounced. When η^{*2} reaches exactly the value $3/4$, there is a departure from the exponential behavior towards a linear growth (neutral limit), while for $\eta^{*2}>3/4$ the TKE stabilizes. However, identifying the true "neutral state" is rather difficult, since no account for viscous dissipation of TKE has been made. In Fig. 3, the evolution of the normalized stresses r_{ij} and the structure dimensionality tensor components d_{ij} (Ref. 1) for the 2D ap-

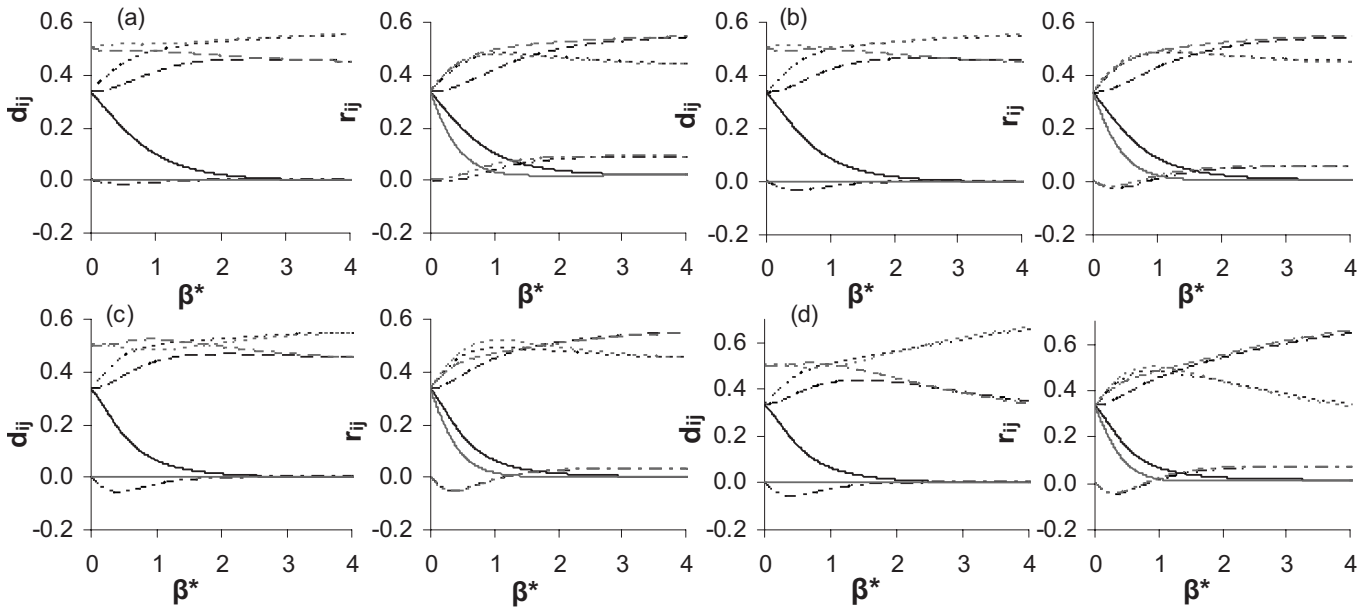

FIG. 3. Comparisons of the evolution of the normalized stresses (right) and the structure dimensionality (left) components 11 (solid), 22 (short dashed), 33 (long dashed), 12 (dotted dashed) for $\eta^{*2}=0.25$ with $\gamma=0.25$ (a), 0.5 (b), 0.75 (c), for $\eta^{*2}=0.64$ with $\gamma=0.75$ (d), for initially isotropic 3D turbulence (black) and 2D with $k_1=0$ (gray).

proximation are illustrated for several η^{*2}, and compared with the respective 3D-PRM exact numerical solutions (in eddy-axes coordinates). Despite the initial differences (at short times, due to the different initializations), the two solutions quickly converge to each other, and for any value of η^{*2} the limiting states reached by the 2D case are the same as the corresponding limiting states for initially 3D isotropic turbulence. As mentioned, the d_{11} component in the 3D solution (in the eddy-axis system) tends quickly to zero, independently of the rotation rate, which is why the 2D solution with $k_1=0$ is a good approximation. For the unstable cases the turbulence evolves fast towards a 2D-3C state, and the final distribution of the TKE among the different stress components, as well as the anisotropy of the dimensionality tensor in the 2D plane, depends on the value of η^{*2}. For the neutral limit and for the stable cases the turbulence evolves towards a fixed 1D-1C state with $r_{33}\rightarrow 1$, $d_{22}\rightarrow 1$. That is, the turbulence appears as sheets perpendicular to the x_2 axis with turbulent velocity fluctuations along the axis of the frame rotation.

This work is dedicated to the late Professor William C. Reynolds. The basic premise of this work was originated by his inspiration. This work has been performed under the UCY-CompSci project, a Marie Curie Transfer of Knowledge (TOK-DEV) grant (Contract No. MTKD-CT-2004-014199) funded by the CEC under the 6th Framework Program and under the WALLTURB project (a European synergy for the assessment of wall turbulence, Contract No. AST4-CT-2005-516008), both funded by the CEC under the 6th Framework Program.

[1] E. Akylas, C. Langer, S. Kassinos, and E. Demosthenous, "On the stability of turbulent plane strain flow in a rotating frame," Phys. Fluids **19**, 075108 (2007).
[2] S. C. Kassinos and W. C. Reynolds, "A structure-based model for the rapid distortion of homogeneous turbulence," Tech. Rep. TF-61, Department of Mechanical Engineering, Stanford University, Stanford, CA, 1994.
[3] S. C. Kassinos and W. C. Reynolds, "A particle representation model for the deformation of homogeneous turbulence," in *Annual Research Briefs* (Stanford University and NASA Ames Research Center, Center for Turbulence Research, Stanford, CA, 1996), pp. 31–50.
[4] S. C. Kassinos and W. C. Reynolds, "Structure-based modeling for homogeneous MHD turbulence," in *Annual Research Briefs* (Stanford University and NASA Ames Research Center, Center for Turbulence Research, Stanford, CA, 1999), pp. 301–315.
[5] G. K. Batchelor, "The effect of homogeneous turbulence on material lines and surfaces," Proc. R. Soc. London, Ser. A **213**, 349 (1952).
[6] S. Goto and S. Kida, "Enhanced stretching of material lines by anti-parallel vortex pairs in turbulence," Fluid Dyn. Res. **33**, 403 (2003).
[7] E. Dresselhaus and M. Tabor, "The kinematics of stretching and alignment of material elements in general flow fields," J. Fluid Mech. **236**, 415 (1991).
[8] E. Akylas, S. C. Kassinos, and C. A. Langer, "Rapid shear of initially anisotropic turbulence in a rotating frame," Phys. Fluids **19**, 025102 (2007).
[9] R. S. Rogallo, "Numerical experiments in homogeneous turbulence," NASA Tech. Memo. 81315, 1981.
[10] S. C. Kassinos, B. Knaepen, and D. Carati, "Passive scalar transport in MHD turbulence sheared in a rotating frame," Phys. Fluids **19**, 015105 (2007).
[11] S. C. Kassinos, W. C. Reynolds, and M. M. Rogers, "One-point turbulence structure tensors," J. Fluid Mech. **428**, 213 (2001).
[12] A. Salhi, C. Cambon, and C. G. Speziale, "Linear stability analysis of plane quadratic flows in a rotating frame with applications to modeling," Phys. Fluids **9**, 2300 (1997).
[13] C. G. Speziale, "Some interesting properties of two-dimensional turbulence," Phys. Fluids **24**, 1425 (1981).